# Dark Matter Dynamics in the Early Universe

by

Lin Fei

Submitted to the Department of Physics
in partial fulfillment of the requirements for the degree of

Bachelor of Science in Physics

at the

MASSACHUSETTS INSTITUTE OF TECHNOLOGY

June 2012



Author .....
Department of Physics
May 13, 2011

Certified by .....
Jesse Thaler
Assistant Professor of Physics
Thesis Supervisor

Accepted by .....
Nergis Mavalvala
Professor, Senior Thesis Coordinator, Department of Physics

# Dark Matter Dynamics in the Early Universe

by

Lin Fei

Submitted to the Department of Physics
on May 13, 2011, in partial fulfillment of the
requirements for the degree of
Bachelor of Science in Physics

## Abstract

We study a new form of dark matter interaction which may significantly affect the thermal relic abundance of dark matter. This new interaction takes the form $C+D \rightarrow C+\phi$, where $D$ is the dark matter species present today, $\phi$ is a standard model species, and $C$ is a very heavy exotic particle. In particular, $C$ was present during the period when freeze-out occured for dark matter species $D$, but subsequently decayed into standard model particles. We refer to this process as a catalytic reaction, since $C$ acts as a catalyst for the destruction of $D$. We further postulate that there is a matter-antimatter asymmetry in $C$, so that $C + \bar{C} \rightarrow D + \phi$ is suppressed. We find that the catalytic reaction produces very different dynamics than the standard annihilation reaction. We also find that the catalytic reaction can significantly affect the relic abundance of dark matter even if it has a much smaller cross section than the annihilation reaction. Possible physical origins for this catalytic reaction are discussed.

Thesis Supervisor: Jesse Thaler
Title: Assistant Professor of Physics

# Acknowledgments

I would like to thank my thesis advisor Professor Jesse Thaler for his clear explanations and valuable comments.

# Contents

# Chapter 1

# Introduction

Many observational evidence across a wide range of scales, such as galactic rotation curves, velocity dispersion of galaxies, and gravitational lensing, all indicate there is missing mass in the universe [1][2][3]. Although some alternative theories of gravity, such as Modified Newtonian Dynamics (MOND) [4], have been proposed to account for this discrepancy, dark matter is still the most popular theory to explain the unobserved mass. However, due to a lack of direct detection evidence, the nature of dark matter remains one of the biggest open problems in modern physics.

Currently, Weakly Interacting Massive Particles (WIMP) are particularly successful dark matter candidates. In the Lee-Weinberg scenario [5], WIMP particles $\psi$ and its anti-particles $\bar{\psi}$ thermalize in the early universe through the annihilation reaction $\psi\bar{\psi} \rightarrow \phi\phi$, where $\phi$ is a standard model degree of freedom. Naively, one would expect the number density of $\psi$ to decrease and eventually reach 0, however, if we take the expansion of the universe into consideration, we find that eventually the interaction rate will be too slow to keep up with the expansion, and the number density asymptotes to a constant. This is referred to as thermal freeze-out.

Boltzmann's equations are necessary to calculate the number density as a function of time in an expanding universe. It is found that in the Lee-Weinberg scenario, if we assume $m_\psi$ is on the order of 100 GeV, and assume an electroweak annihilation cross section, we roughly obtain the observed abundance for dark matter. Physicists refer to this as the "WIMP miracle".

In this paper, we postulate the existence of a new exotic particle $C$ that participates in dark matter dynamics. For the bulk of the paper, we will not specify the properties of $C$, but we will argue that this "catalyst" field can arise in supersymmetric theories. We will demonstrate that, if we assume a catalytic reaction can occur via $C + D \to C + \phi$ (where $D$ is the dark matter species, and $C$ the "catalyst") in addition to the annihilation reaction $D + \bar{D} \to \phi\phi$, the thermal relic abundance can be significantly altered even if the catalytic cross section is much smaller. The catalytic process is an extreme limit of the so-called "semi-annihilation" process studied in [6]. In our catalytic scenario, we will assume that there is an asymmetry in $C$ and its anti-particle $\bar{C}$, so that $C + \bar{C} \to D + \phi$ is suppressed. For simplicity, we will assume the number density of $\bar{C}$ is 0, ie $C$ and $\bar{C}$ have annihilated as much as possible before $D$ freezes out. Since the baryon asymmetry is on the order of $n/s = 6.23(17) \times 10^{-10}$ [7], we will assume $n_C/s = 10^{-9}$, where $s$ is the entropy density per comoving volume.

The rest of the paper is organized as follows. In section 2, we introduce and derive the general Boltzmann's equation in an expanding universe. In section 3, we recast the general Boltzmann's equation specifically for the annihilation and catalytic reactions. In section 4, we solve the Boltzmann's equation derived previously with the catalytic reaction turned off, so it will be the same as the standard Lee-Weinberg scenario. We will present both the numerical and semi-analytic solution to the equation, and calculate the cross section of the annihilation reaction necessary to yield the observed thermal relic abundance for dark matter. In section 5, we will solve the Boltzmann's equation with only the catalytic reaction both numerically and analytically, and find the cross section of the catalytic reaction that will yield the observed abundance. In section 6, we turn on both the annihilation and catalytic reactions and solve the Boltzmann's equation numerically, and discuss how their combined effect affects dark matter relic abundance. In section 7, we will discuss how catalytic reactions can occur in supersymmetric theories, and how it can impact the dark matter relic abundance. Finally, we will conclude and discuss future works in section 8.

# Chapter 2

# Boltzmann Equation

In the early universe, many particle species can collide and produce different species. We can employ statistical mechanics and describe each species with a phase space density $f(\vec{x},\vec{p},t)$. The phase space density is related to the actual number density as:

$$n(t) = \frac{g}{(2\pi)^3}\int d^3p f(\vec{x},\vec{p},t) \ , \tag{2.1}$$

where $g$ is the internal degree of freedom of the particle.

The evolution of a species' number density in the presence of various interactions is given by the Boltzmann Equation, whose most general form is:

$$\hat{L}[f] = C[f] \ , \tag{2.2}$$

where $\hat{L}$ is the Liouville operator and $C$ is the collision operator. The covariant generalization of the Liouville operator in general relativity can be written as:

$$\hat{L} = p^\alpha \frac{\partial}{\partial x^\alpha} - \Gamma^\alpha_{\beta\gamma} p^\beta p^\gamma \frac{\partial}{\partial p^\alpha} \ , \tag{2.3}$$

Where $\Gamma^\alpha_{\beta\gamma}$ is the connection. If we use the Robertson-Walker metric: $ds^2 = dt^2 - R^2(t)[dr^2 + r^2 d\theta^2 + r^2 \sin^2\theta d\phi^2]$, and assume the dependence of $f$ on momentum is

isotropic, the above operator becomes:

$$\hat{L}[f(E,t)] = E\frac{\partial f}{\partial t} - Hp^2\frac{\partial f}{\partial E}\ , \tag{2.4}$$

where $H \equiv \dot{R}/R$ is the Hubble parameter, and $E^2 = p^2 + m^2$. Using integration by parts, it is then possible to rewrite the Boltzmann equation in terms of the number density $n$ as:

$$\frac{dn}{dt} + 3\frac{\dot{R}}{R}n = \frac{g}{(2\pi)^3}\int C[f]\frac{d^3p}{E}\ . \tag{2.5}$$

Notice that in the absence of the collision term, the above equation becomes: $\dot{n}R + 3\dot{R}n = 0$, or $nR^3 = \text{const}$, which is to say that $n$ decreases as $R^3$ as the universe expands, which is indeed what we expect.

The collision term is the sum of many processes. For a particular process $1+2 \longleftrightarrow 3+4$, the collision term is:

$$\begin{aligned}\frac{g}{(2\pi)^3}\int C[f]\frac{d^3p}{E} = \int \frac{d^3p_1}{(2\pi)^3 2E_1}\int \frac{d^3p_2}{(2\pi)^3 2E_2}\int \frac{d^3p_3}{(2\pi)^3 2E_3}\int \frac{d^3p_4}{(2\pi)^3 2E_4} \\ \times (2\pi)^4\delta^3(p_1+p_2-p_3-p_4)\delta(E_1+E_2-E_3-E_4)|\mathcal{M}|^2 \\ \times \{f_3 f_4[1\pm f_1][1\pm f_2] - f_1 f_2[1\pm f_3][1\pm f_4]\}\ ,\end{aligned} \tag{2.6}$$

Note that we have suppressed $\hbar$ in the equation above. Each $f_i$ in the above equation in fact denotes $f_i(\vec{x},\vec{p},t)$. The amplitude $|\mathcal{M}|$ is determined by the physics involved in the process. Here, we assumed both the forward and backward reactions have the same amplitude, which is true given CP invariance. The integrals are over the 4-momenta of particles 1,2,3,4. However, since we need to impose $E^2 = p^2 + m^2$, the 4-momentum integrals become:

$$\int d^3p\int_0^\infty dE\delta(E^2-p^2-m^2) = \int d^3p\int_0^\infty dE\frac{\delta(E-\sqrt{p^2-m^2})}{2E} = \int\frac{d^3p}{2E}\ . \tag{2.7}$$

Finally, other than the $[1\pm f]$ terms, the last line says that the rate of producing species 1 is proportional to $f_3 f_4$, while the rate of depleting species 1 is proportional to $f_1 f_2$. The $[1\pm f]$ terms account for Bose enhancement and Pauli blocking.

If we assume the particles are in equilibrium, the phase space distribution will be given by either the Bose-Einstein distribution or the Fermi-Dirac distribution, for bosons and fermions respectively:

$$f = \frac{1}{e^{(E-\mu)/T} \pm 1} , \tag{2.8}$$

with the plus sign for fermions and minus sign for bosons, and where $\mu$ is the chemical potential. Typically, we are interested in regions where $T \ll E - \mu$, so we can approximate (2.8) as $f = e^{\mu/T} e^{-E/T}$. We can also safely ignore the Bose enhancement and Pauli blocking terms in this limit, so the last line of (2.6) becomes:

$$f_3 f_4 [1 \pm f_1][1 \pm f_2] - f_1 f_2 [1 \pm f_3][1 \pm f_4] \tag{2.9}$$

$$= e^{-(E_3+E_4)/T} e^{(\mu_3+\mu_4)/T} - e^{-(E_1+E_2)/T} e^{(\mu_1+\mu_2)/T} \tag{2.10}$$

$$= e^{-(E_1+E_2)/T} [e^{(\mu_3+\mu_4)/T} - e^{(\mu_1+\mu_2)/T}] , \tag{2.11}$$

where we used $E_1 + E_2 = E_3 + E_4$ to get to the last line. So far, this is an expression involving the chemical potentials $\mu_i$. We can turn it into an equation involving the number density as follows. First, recall that:

$$n_i = \frac{g}{(2\pi)^3} \int d^3p f_i(\vec{x}, \vec{p}, t) \tag{2.12}$$

$$= g_i e^{\mu_i/T} \int \frac{d^3p}{(2\pi)^3} e^{-E_i/T} . \tag{2.13}$$

This allows us to write $e^{\mu_i/T} = n_i / n_i^{eq}$ where we have defined the equilibrium density to be:

$$n_i^{eq} = g \int \frac{d^3p}{(2\pi)^3} e^{-E_i/T} . \tag{2.14}$$

The equilibrium density is the density when the chemical potential is 0, ie. if the particle is in thermal equilibrium with its surroundings.

Using this, (2.11) can now be written as:

$$e^{(-E_1+E_2)/T} \left[ \frac{n_3 n_4}{n_3^{eq} n_4^{eq}} - \frac{n_1 n_2}{n_1^{eq} n_2^{eq}} \right] . \tag{2.15}$$

Notice that this term is independent of $p$ so we can take it out of the integral. Defining the thermal averaged cross section to be:

$$\langle \sigma v \rangle \equiv \frac{1}{n_1^{eq} n_2^{eq}} \int \frac{d^3p_1}{(2\pi)^3 2E_1} \int \frac{d^3p_2}{(2\pi)^3 2E_2} \int \frac{d^3p_3}{(2\pi)^3 2E_3} \int \frac{d^3p_4}{(2\pi)^3 2E_4} ,$$
$$e^{-(E_1+E_2)/T} (2\pi)^4 \delta^3(p_1 + p_2 - p_3 - p_4) \delta(E_1 + E_2 - E_3 - E_4) |M|^2 , \qquad (2.16)$$

we finally arrive at the following form for the Boltzmann equation:

$$\frac{dn_1}{dt} + 3Hn_1 = n_1^{eq} n_2^{eq} \langle \sigma v \rangle \left[ \frac{n_3 n_4}{n_3^{eq} n_4^{eq}} - \frac{n_1 n_2}{n_1^{eq} n_2^{eq}} \right] . \qquad (2.17)$$

When there are multiple interactions changing the density of $n_1$, we simply add more terms to the right hand side of the above equation.

# Chapter 3

# Boltzmann Equation for the Annihilation and Catalytic Reactions

Now we are ready to write the Boltzmann equation for our specific toy model.

Recall that in the Lee-Weinberg scenario, the dark matter species $D$ annihilates via the reaction $D + \bar{D} \rightarrow \phi + \phi$, where $\phi$ is a standard model particle. Standard model particles are much lighter than $C$ or $D$, so they will remain in contact with the background temperature for much longer, so we can assume $n_\phi = n_\phi^{eq}$.

In addition, we will postulate the existence of another exotic heavy particle $C$, which can lower the density of $D$ via $C + D \rightarrow C + \phi$, and $C + \bar{D} \rightarrow C + \phi$. Since $C$ is very massive, it froze out way before $D$. We further assume that there is a matter-antimatter asymmetry in $C$, which causes the anti-particle $\bar{C}$ to be completely annihilated, leaving $C$ at a constant density during the freeze-out of $D$. The lack of $\bar{C}$ prevents the creation of $D$ via processes such as $C + \bar{C} \rightarrow D + \phi$. Hence, $C$'s only role is to serve as a "catalyst" to decrease the abundance of $D$. We will investigate when the catalytic reaction will be significant compared to the annihilation reaction.

There are three processes in this toy model:

$$C + D \to C + \phi \,, \tag{3.1}$$

$$C + \bar{D} \to C + \phi \,, \tag{3.2}$$

$$D + \bar{D} \to \phi + \phi \,. \tag{3.3}$$

Assuming CP invariance, the cross-section of (3.1) and (3.2) are the same. This symmetry in $D$,$\bar{D}$ ensures that they have the same abundance, we can treat it as a single variable $n_D$. From (2.17) the Boltzmann equation is:

$$\frac{dn_D}{dt} + 3Hn_D = \mathcal{C}^{cat} + \mathcal{C}^{ann} \,, \tag{3.4}$$

where the collision terms are:

$$\mathcal{C}^{cat} = -\langle \sigma v \rangle_{CD \to C+\phi} [n_C n_D - n_C n_D^{eq}] \,, \tag{3.5}$$

$$\mathcal{C}^{ann} = -\langle \sigma v \rangle_{D\bar{D} \to \phi\phi} [n_D^2 - n_D^{eq2}] \,. \tag{3.6}$$

We only consider $s$-wave cross sections and assume that both $\langle \sigma v \rangle$ are constant through time for simplicity.

We redefine the variables as:

$$Y_D \equiv \frac{n_D}{s} \,, \tag{3.7}$$

$$x \equiv \frac{m_D}{T} \,, \tag{3.8}$$

$$\lambda_1 \equiv \frac{s(x=1)}{H(x=1)} \langle \sigma v \rangle_{CD \to C\phi} \,, \tag{3.9}$$

$$\lambda_2 \equiv \frac{s(x=1)}{H(x=1)} \langle \sigma v \rangle_{D\bar{D} \to \phi\phi} \,, \tag{3.10}$$

where $s$ is the entropy density per co-moving volume, which satisfies $sR^3 = const.$

Hence

$$\frac{ds}{dt}R^3 + 3Rs\frac{dR}{dt} = 0 \ , \tag{3.11}$$

$$\frac{ds}{dt} = -3s\frac{dR/dt}{R} = -3sH \ . \tag{3.12}$$

Notice that since $n_D = sY_D$, we have

$$\frac{dn_D}{dt} = s\frac{dY_D}{dt} + Y\frac{ds}{dt} \tag{3.13}$$

$$= s\frac{dY_D}{dt} - 3HsY \tag{3.14}$$

$$= s\frac{dY_D}{dt} - 3Hn_D \ , \tag{3.15}$$

so the left-hand-side of Boltzmann Equation (3.4) becomes $s\frac{dY_D}{dt}$, and we end up with:

$$s\frac{dY_D}{dt} = -\left\langle \sigma v \right\rangle_{CD\to C\phi}\left[n_C n_D - n_C n_D^{eq}\right] - \left\langle \sigma v \right\rangle_{D\bar{D}\to\phi\phi}\left[n_D^2 - n_D^{eq2}\right] \ . \tag{3.16}$$

Dividing both sides of the above equation by $s$, we get:

$$\frac{dY_D}{dt} = -s\left\langle \sigma v \right\rangle_{CD\to C\phi}\left[Y_C Y_D - Y_C Y_D^{eq}\right] - s\left\langle \sigma v \right\rangle_{D\bar{D}\to\phi\phi}\left[Y_D^2 - Y_D^{eq2}\right] \ . \tag{3.17}$$

Now we need to change the time variable from $t$ to $x = m/T$. In the radiation-dominated epoch, equation (5.15) of [8] gives:

$$t = 0.301 g_*^{-1/2}\frac{m_{pl}}{m^2}x^2 \ , \tag{3.18}$$

Where $g_*$ counts the total number of effective massless degrees of freedom, and is defined in equation 3.62 of [8], and $m_{pl}$ is the Planck mass. So we have

$$\frac{dt}{dx} = 0.602 g_*^{-1/2}\frac{m_{pl}}{m^2}x$$

$$= \frac{x}{H(m)} \ , \tag{3.19}$$

Where $H(m) = H(x=1) = 1.67 g_*^{1/2} \frac{m^2}{m_{pl}}$, from equation 5.16 of [8].

So, after changing variable from $t$ to $x$, the Boltzmann equation becomes:

$$\frac{dY_D}{dx} = -\frac{s\langle\sigma v\rangle_{CD\to C\phi}}{H(x=1)\frac{1}{x}}[Y_C Y_D - Y_C Y_D^{eq}] - \frac{s\langle\sigma v\rangle_{D\bar{D}\to\phi\phi}}{H(x=1)\frac{1}{x}}[Y_D^2 - Y_D^{eq2}] \,. \tag{3.20}$$

Now from equation 3.72 of [8]:

$$s = \frac{2\pi^2}{45} g_{*s} T^3 = \frac{2\pi^2}{45} g_{*s} \frac{m^3}{x^3} = \frac{s(x=1)}{x^3} \,, \tag{3.21}$$

where $g_{*s}$ counts the contribution of relativistic particles to the entropy density, and is defined in equation 3.73 of [8], so the Boltzmann equation becomes:

$$\frac{dY_D}{dx} = -\frac{s(x=1)\langle\sigma v\rangle_{CD\to C\phi}}{H(x=1)x^2}[Y_C Y_D - Y_C Y_D^{eq}] - \frac{s(x=1)\langle\sigma v\rangle_{D\bar{D}\to\phi\phi}}{H(x=1)x^2}[Y_D^2 - Y_D^{eq2}] \,, \tag{3.22}$$

or, using the definition of $\lambda$,

$$\frac{dY_D}{dx} = -\frac{1}{x^2}\left[\lambda_1[Y_C Y_D - Y_C Y_D^{eq}] + \lambda_2[Y_D^2 - Y_D^{eq2}]\right] \,, \tag{3.23}$$

where

$$Y_D^{eq} = \frac{g_D}{g_{*s}} \frac{45}{4\pi^4} x^2 K_2[x] \tag{3.24}$$

is the equilibrium density, and $K_2[x]$ is the modified Bessel function of the second kind. For the remainder of the paper, we will assume $g_D = 1$, $g_{*s} = 100$ (which is typical in the early universe see Fig. 3.5 in [8]), so $Y_D^{eq} = \frac{45}{400\pi^4} x^2 K_2[x]$.

# Chapter 4

# Solving Boltzmann Equation in the Lee-Weinberg Scenario

Equation (3.23) has both the standard annihilation term and the new catalytic term. In this section we will study just the annihilation piece. If we only keep the annihilation term, the Boltzmann equation (3.23) becomes

$$\frac{dY_D}{dx} = -\frac{1}{x^2}\lambda_2[Y_D^2 - Y_D^{eq2}] \, . \tag{4.1}$$

We can solve this differential equation numerically and obtain the freeze-out density $Y_D(\infty)$. For our numerical studies, we will assume $m_D = 100$ GeV.

To convert the dimensionless $Y_D(\infty)$ into a meaningful dark matter abundance, we use equation (5.46) of [8], where the dark matter number density today is $n_{D0} = s_0 Y_\infty = 2970 Y_\infty \text{cm}^{-3}$,

$$\begin{aligned} \Omega_D h^2 &= \frac{n_{D0} \times m_D}{1.055 \times 10^{-5} \text{GeV/cm}^3} \\ &= 2.815 \times 10^8 Y_\infty m_D \text{GeV}^{-1} \\ &= 2.815 \times 10^{10} Y_\infty \, . \end{aligned} \tag{4.2}$$

Here, $\Omega_D h^2$ is the abundance of dark matter, which is the ratio between the dark matter mass density and the critical density $\rho_{cr} = \frac{3H_0}{8\pi G}$. Similarly, we also need to

turn $\lambda$ into a cross section $\langle\sigma v\rangle$. From (3.10):

$$\lambda = \frac{\langle\sigma v\rangle\, s(x=1)}{H(x=1)}\ , \tag{4.3}$$

where $s(x=1) = \frac{2\pi^2}{45} g_{*s} m^3$ from equation (3.72) of [8], $H(x=1) = 1.66\sqrt{g_*}\frac{m^2}{m_{pl}}$ from equation 3.63 of [8], thus

$$\lambda = 0.264 \frac{g_{*s}}{\sqrt{g_*}} m_{pl} m \langle\sigma v\rangle\ . \tag{4.4}$$

Assuming $g_{*s} = g_* = 100$,

$$\langle\sigma v\rangle = \frac{0.379\lambda}{m_{pl} m}\ . \tag{4.5}$$

We are working in units where $\hbar = c = 1$. So we need to put in the appropriate factors of $\hbar$ and $c$ to make the equation dimensionally correct. Notice that $\lambda$ is dimensionless, and $\langle\sigma v\rangle$ has a dimension of $\mathrm{cm}^2$, so we have:

$$\langle\sigma v\rangle = \frac{0.379\hbar^2 c^2}{m_{pl} m}\lambda\ . \tag{4.6}$$

With $m_{pl} = 1.221 \times 10^{19}\mathrm{GeV}$, $m = 100$ GeV, we get:

$$\langle\sigma v\rangle = 1.209 \times 10^{-49}\lambda \mathrm{cm}^2\ . \tag{4.7}$$

Solving the Boltzmann equation numerically, and converting all the dimensionless quantities into meaningful quantities with the two conversion formulae above, it is found that, to have $\Omega_D h^2 = 0.1$, (the 95% CL is determined to be between 0.0975 and 0.1223 [9]) we want $\lambda_2 \approx 6 \times 10^{12}$, which corresponds to $\langle\sigma v\rangle = 0.73$ pb.

Figure 4-1 is a plot of $Y_D$ vs $x$ obtained numerically.

## 4.1 Semi-Analytic Solution Using Freeze-out

Notice that there is a very distinctive value of $x_f$ ($\approx 20$) when freeze-out occurs, namely when $Y_D$ deviates from $Y_D^{eq}$. $Y_D$ was in equilibrium and follows closely with

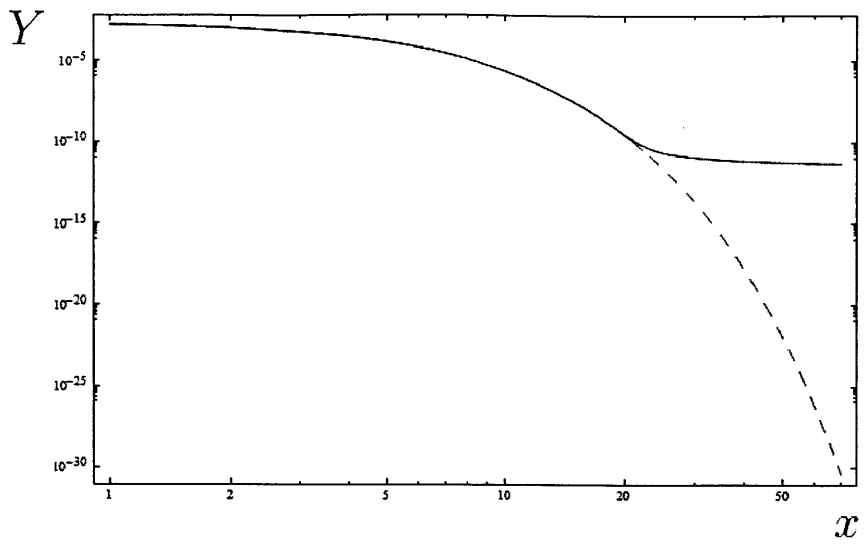


Figure 4-1: Annihilation reaction with $\lambda_2 = 6 \times 10^{-12}$. The dashed line represents $Y_D^{eq}$, and the solid line is $Y_D$.

$Y_D^{eq}$ for $x < x_f$, then, $Y_D$ suddenly freezes out at $x > x_f$.

Using this feature, it is possible to derive a fairly accurate semi-analytic solution to the Boltzmann equation in the Lee-Weinberg scenario. First, we define $Q(x) \equiv Y_D(x) - Y_D^{eq}(x)$, and consider the differential equation satisfied by $Q(x)$:

$$\frac{dQ}{dx} = -\frac{dY_D^{eq}}{dx} - \frac{\lambda_2}{x^2} Q(2Y_D^{eq} + Q) \; . \tag{4.8}$$

In the region where $x \ll x_f$, $Y_D$ is very close to $Y_D^{eq}$, so both $Q$ and $dQ/dx$ are very close to 0. It turns out that it is a good approximation to set $dQ/dx = 0$ in this region, so we have:

$$\begin{aligned} Q &\approx -\frac{x^2}{\lambda_2} \frac{dY_D^{eq}/dx}{2Y_D^{eq} + Q} \\ &\approx -\frac{x^2}{2\lambda_2} \frac{dY_D^{eq}/dx}{Y_D^{eq}} \; . \end{aligned} \tag{4.9}$$

For $x > 3$ we can approximate $Y_D^{eq} \approx 0.145 \frac{g}{g_{*S}} x^{3/2} e^{-x}$ using equation 5.25 of [1], such

that:

$$\frac{dY_D^{eq}/dx}{Y_D^{eq}} = (3/2x - 1) \approx -1 \ , \tag{4.10}$$

for $x$ big enough. Combining (4.9) and (4.10), we obtain that for $x < x_f$,

$$Q(x) \approx \frac{x^2}{2\lambda_2} \ . \tag{4.11}$$

Now, when $x > x_f$, $Y_D^{eq}$ is exponentially suppressed, so $Q \gg Y_D^{eq}$, and the differential equation for $Q(x)$ becomes:

$$Q' = -\frac{\lambda_2}{x^2}Q^2 \ . \tag{4.12}$$

Suppose $Q(x_f) = \Delta$, we can integrate the above equation to find:

$$-\frac{1}{Q(x)} + \frac{1}{\Delta} = \lambda_2 \left(\frac{1}{x} - \frac{1}{x_f}\right) \ . \tag{4.13}$$

Typically, $\Delta \gg Q(x)$, so we can ignore the second term on the left-hand-side. When $x = \infty$, we get:

$$Q(\infty) = Y_D(\infty) = \frac{x_f}{\lambda_2} \ . \tag{4.14}$$

Notice that if we have $x_f$, we have $Y_D(\infty)$.

[8] provides a procedure to find $x_f$ as follows: first, define $x_f$ by the criterion $Q(x_f) = cY_D^{eq}(x_f)$, where $c$ is a constant of order unity. Substituting in the early solution of $Q(x) = x_f^2/\lambda_2(2+c)$ gives:

$$x_f \approx \ln[(2+c)\lambda_2 ac] - \frac{1}{2}\ln[\ln[(2+c)\lambda_2 ac]] \ , \tag{4.15}$$

where $a = 0.145g/g_{*S} = 0.00145$. Here we pick $c = 1 + \sqrt{2} = 2.414$. If we choose $\lambda_2 = 6 \times 10^{12}$, we get $x_f = 23.6$. And hence $Y_D(\infty) = 3.93 \times 10^{-12}$, which corresponds to $\Omega_D h^2 = 0.112$. Recall that we found numerically $Y_D(\infty) = 0.100$ with the same $\lambda_2$, we see that the semi-analytic solution gives a very accurate answer. Figure 4-2 compares the numerical and analytic solutions of $Q(x)$

Figure 4-3 is a graph that shows how the relic abundance changes as a function of $\lambda_2$. Notice that the vertical scale is the logarithm of $\Omega_D h^2$, a relic abundance of

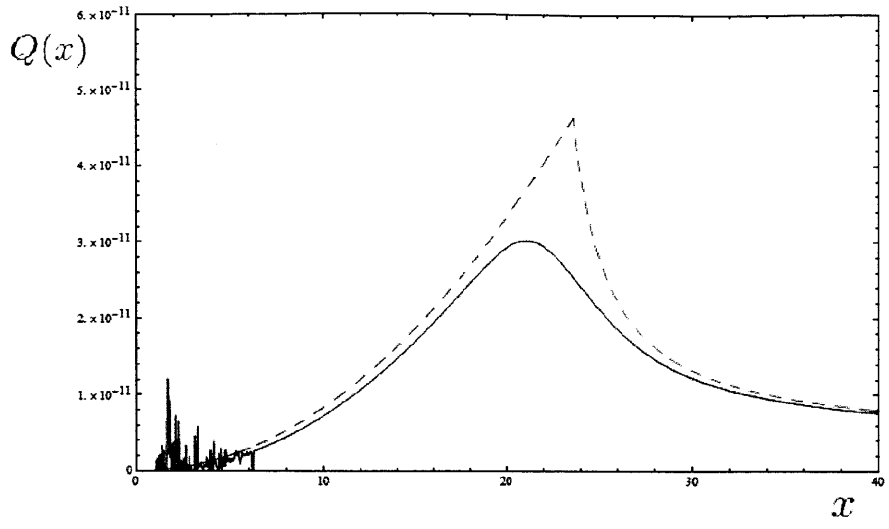


Figure 4-2: Numerical (solid) vs semi-analytic (dashed) solution of $Q(x)$ in the annihilation reaction. The semi-analytic solution is obtained by piecing together the analytic solutions for $x \ll x_f$ and $x \gg x_f$ at $x_f$.

0.1 would correspond to a value of $-1$.

To summarize, we find that with $m_D = 100$ GeV, the cross section of the annihilation reaction should be $\langle \sigma v \rangle = 0.73$ pb to yield a relic abundance of $\Omega_D h^2 = 0.100$. As the cross section increases, $\Omega_D h^2$ decreases roughly as $1/\lambda_2$.

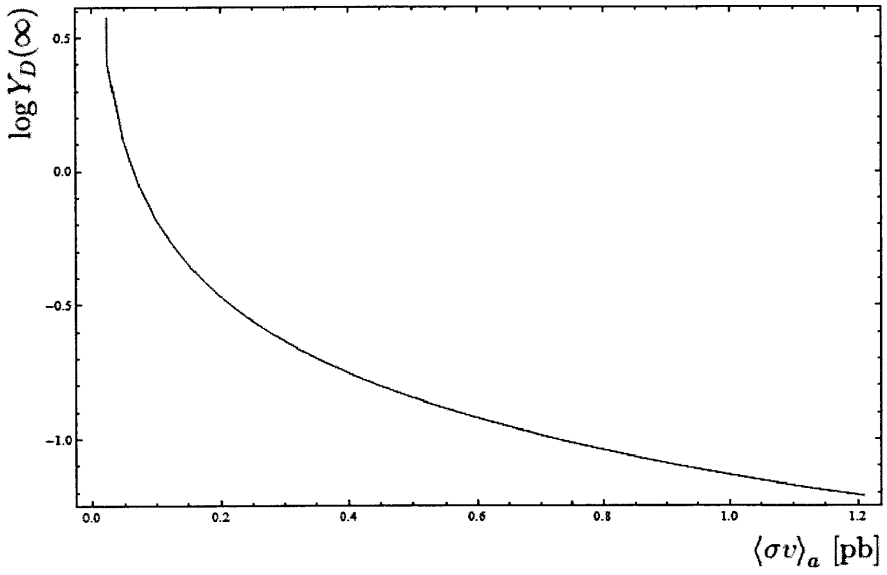


Figure 4-3: Log of relic abundance vs annihilation cross section 0 to 1.2 pb.

# Chapter 5

# Boltzmann Equation with Catalytic Reaction

Having understood the standard freeze-out calculation, we now turn to the new catalytic reaction. When only the catalytic reaction is possible, we can set $\lambda_2 = 0$ in the Boltzmann equation, yielding

$$\frac{dY_D}{dx} = -\frac{1}{x^2}\lambda_1 Y_C[Y_D - Y_D^{eq}] \ . \tag{5.1}$$

For convenience, we define $\Lambda \equiv \lambda_1 Y_C$ where $Y_C = 10^{-9}$, so

$$\frac{dY_D}{dx} = -\frac{\Lambda}{x^2}[Y_D - Y_D^{eq}] \ . \tag{5.2}$$

Note that the solution only depends on the combination $\Lambda = \lambda_1 Y_C$. We will see that in order to yield a thermal relic abundance of 0.1, $\Lambda$ is typically on the order of 150. Figure 5-1 is a numerical solution of $Y_D$ with $\Lambda = 100$.

Comparing this solution with the annihilation solution, we see that the freeze-out is less well defined in the catalytic case, i.e. the number density of dark matter continues to decrease even after it has been detached from the equilibrium solution. Thus, to calculate the abundance, we need to evaluate the solution at a sufficiently late time.

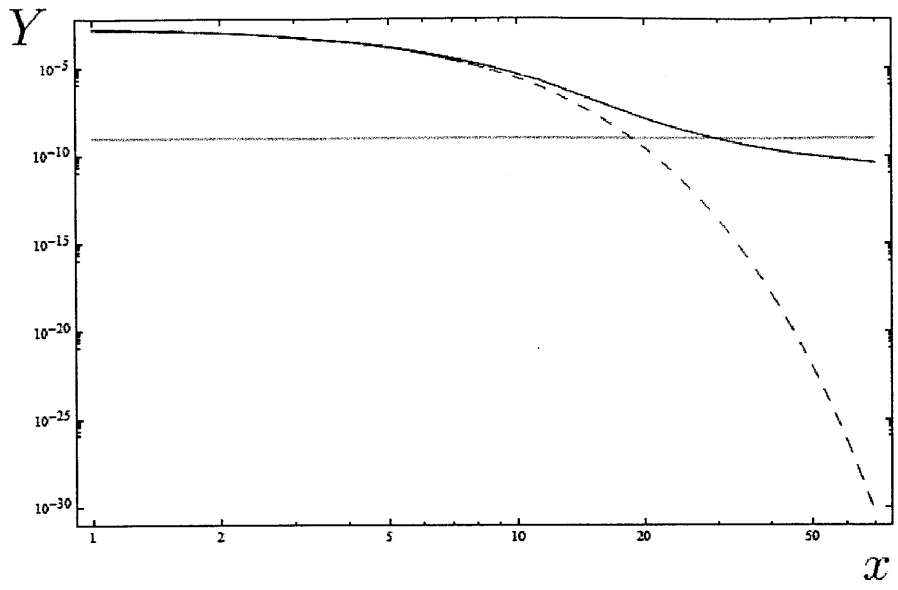


Figure 5-1: Catalytic reaction with $\Lambda = 100$. The dashed line represents $Y_D^{eq}$, the solid line represents $Y_D$. $Y_C$, which is a constant, is also plotted on the graph.

More concretely, at a time when $Y_D \gg Y_D^{eq}$, the Boltzmann equation becomes:

$$\frac{dY_D}{dx} = -\frac{\Lambda}{x^2} Y_D \ . \tag{5.3}$$

The solution to the above equation is $Y_D = Ae^{\Lambda/x}$. This is a much slower decreasing function of $x$ than the annihilation case. Since $\Lambda \approx 100$, even if we take $x = 100$, freeze-out still hasn't technically occured, since the ratio

$$\frac{Y_D(100)}{Y_D(\infty)} = \frac{Ae^{100/100}}{Ae^{100/\infty}} = e \ , \tag{5.4}$$

the true freeze-out level is still another factor of $e$ away! This is very different from the behavior of freeze-out with only annihilation, where $Y_D$ stabilizes shortly after $x_f$. Now, notice that (5.2) is a linear first order equation, so we can solve it exactly.

Analogous to the annihilation case, we define the difference $Q(x) = Y_D(x) - Y_D^{eq}(x)$, so (5.2) becomes:

$$\frac{dQ}{dx} = -\frac{\Lambda}{x^2} Q - \frac{dY_D^{eq}}{dx} \ . \tag{5.5}$$

Since it is a linear equation, its general solution can be broken into two parts: the

homogeneous solution to the differential equation is $Q_H$:

$$\frac{dQ_H}{dx} = -\frac{\Lambda}{x^2} Q_H \ , \tag{5.6}$$

this is easily solved to be $Q_H(x) = Ae^{\Lambda/x}$. The particular solution $Q_P$, to the equation satisfies:

$$\frac{dQ_P}{dx} = -\frac{\Lambda}{x^2} Q_P - \frac{dY_D^{eq}}{dx} \ . \tag{5.7}$$

The general solution is thus: $Q(x) = Q_H(x) + Q_P(x) = Ae^{\Lambda/x} + Q_P(x)$

To solve for $Q_P(x)$, we use the method of integrating factors to obtain:

$$Q_P(x) = -e^{\frac{\Lambda}{x}} \int_1^x \frac{dY_D^{eq}}{du} e^{-\frac{\Lambda}{u}} du \ , \tag{5.8}$$

so the general solution is: $Q(x) = Ae^{\Lambda/x} - e^{\frac{\Lambda}{x}} \int_1^x \frac{dY_D^{eq}}{du} e^{-\frac{\Lambda}{u}} du$. To determine the constant $A$ we impose the boundary condition of $Q(1) = 0$ (since we started our numerical integration at $x = 1$, and at that point we assumed particle $D$ is still completely in thermal equilibrium). But $Q(1) = Ae^{\Lambda} - 0 = 0$, so $A = 0$. Thus the solution to our differential equation is:

$$Q = -e^{\frac{\Lambda}{x}} \int_1^x \frac{dY_D^{eq}}{du} e^{-\frac{\Lambda}{u}} du \ . \tag{5.9}$$

If we are interested in the freeze-out density: $Y_D(\infty) = Q(\infty) + Y_D^{eq}(\infty) = Q(\infty)$

We can make the above expression look nicer using integration by parts:

$$\begin{aligned} Q(\infty) &= -e^{\frac{\Lambda}{x}} \int_1^{\infty} \frac{dY_D^{eq}}{du} e^{-\frac{\Lambda}{u}} du \\ &= -\left[ Y_D^{eq} e^{-\frac{\Lambda}{x}} \right]_1^{\infty} + \int_1^{\infty} Y_D^{eq} \frac{\Lambda}{u^2} e^{-\frac{\Lambda}{u}} du \\ &= \int_1^{\infty} Y_D^{eq} \frac{\Lambda}{u^2} e^{-\frac{\Lambda}{u}} du \ . \end{aligned} \tag{5.10}$$

Now, since $Y_D^{eq} = \frac{g}{g_{*S}} \frac{45}{4\pi^4} x^2 K_2[x]$, we have

$$Q(\infty) = \frac{g}{g_{*S}} \frac{45}{4\pi^4} \Lambda \int_1^{\infty} K_2[u] e^{-\frac{\Lambda}{u}} du \ . \tag{5.11}$$

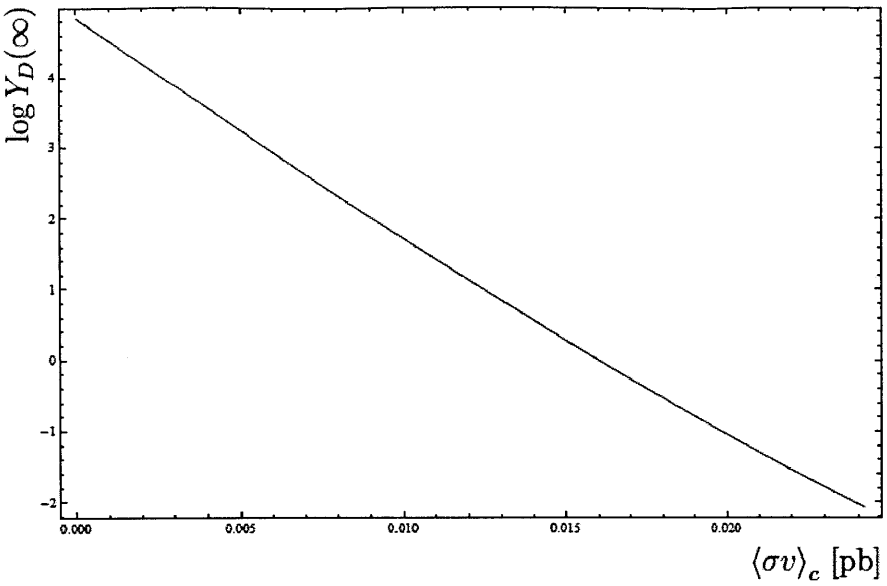


Figure 5-2: Log of relic abundance vs catalytic cross section (0 to 0.0242 pb). This shows that the relic abundance decreases exponentially as $\Lambda$.

We can verify that (5.11) agrees precisely with the numerical solution to the Boltzmann equation.

Figure 5-2 shows the log of the dark matter abundance as a function of the catalytic cross section. The horizontal axis is cross section ranging linearly from 0 to 0.0242 picobarn.

To summarize, the catalytic reaction produces a very different history of dark matter density compared to the annihilation reaction. Firstly, it takes a much longer time for the dark matter density to stablize. Secondly, with a very small cross section of about 0.02 pb, the catalytic reaction is able to achieve the same $\Omega_D h^2$ as the annihilation reaction, which had a cross section of 0.73 pb. Lastly, while $\Omega_D h^2$ only decreases as $1/\lambda_2$ for the annihilation reaction, it decreases exponentially as $\lambda_1$ in the catalytic reaction.

# Chapter 6

# Combined Effect of Annihilation and Catalytic Reaction

Now we want to understand the case where both the annihilation and catalytic reactions are turned on. Figure 6-1 is obtained when we vary the annihilation cross-section along the vertical axis and vary the catalytic cross section along the horizontal axis.

The value of the plot is the log (base 10) of the dark matter abundance $\Omega_D h^2$, where the experimentally determined value of 0.1, which roughly corresponds to a value of -1 on the plot.

Notice that a catalytic reaction with a cross section 50 times smaller than the annihilation reaction has a similar effect on the dark matter relic abundance.

Amazingly, if we estimate the annihilation and catalytic cross sections to be $\langle \sigma v \rangle_c \propto \frac{1}{m_C m_D}$ and $\langle \sigma v \rangle_a \propto \frac{1}{m_D^2}$, we roughly get the correct ratio between the cross sections. It would be interesting to have an explicit physical model which realizes this possibility.

Now, let's study what happens to the dark matter abundacne vs. catalytic cross section curve (Figure 5-2) changes when we introduce a small amount of annihilation reaction. Fix $\langle \sigma v \rangle_a = 0.12$ pb and vary $\langle \sigma v \rangle_c$ from 0 to 0.06 pb, then compare with the case when no annihilation is introduced. The result is shown in Figure 6-2. We see that when $\langle \sigma v \rangle_c$ is large enough, the two lines converge, since the effect of catalytic reaction dominates the annihilation reaction. Similarly, let's fix $\langle \sigma v \rangle_c = 0.0012$ pb

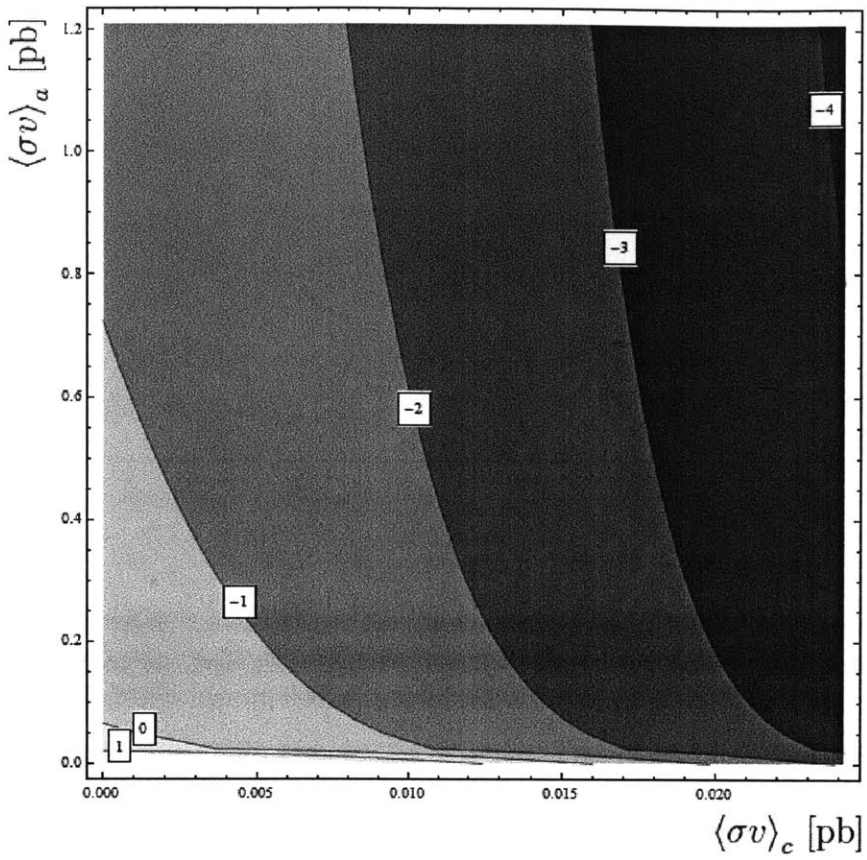


Figure 6-1: Variation of dark matter abundance with $\langle\sigma v\rangle_a$ and $\langle\sigma v\rangle_c$. The observed abundance of $\Omega_D h^2 \simeq 0.10$ corresponds roughly to $-1$ on the graph. The effects of the annihilation and catalytic reactions on the abundance are comparable even though the range of the annihilation cross section is 50 times bigger.

(a very small value), and vary $\langle\sigma v\rangle_a$ from 0 to 60 pb (an extremely large value), and compare this to the same graph without the additional $\langle\sigma v\rangle_c$. We obtain Figure 6-3. Surprisingly, even when $\langle\sigma v\rangle_a$ is absurdly large, the tiny amount of $\langle\sigma v\rangle_c$ is still significant enough to cause a difference in the final abundance. This demonstrates the following fact when we have both the annihilation and catalytic reactions: even a small catalytic cross section will have a noticeable effect on the final abundance of dark matter no matter how big the annihilation cross section is.

This can be understood intuitively as follows: when the annihilation cross section is very large, the dark matter abundance will eventually become very small. When this happens, the annihilation reaction is suppressed as $Y_D^2$, whereas the catalytic reaction is only suppressed as $Y_D$, so the catalytic reaction will eventually dominate

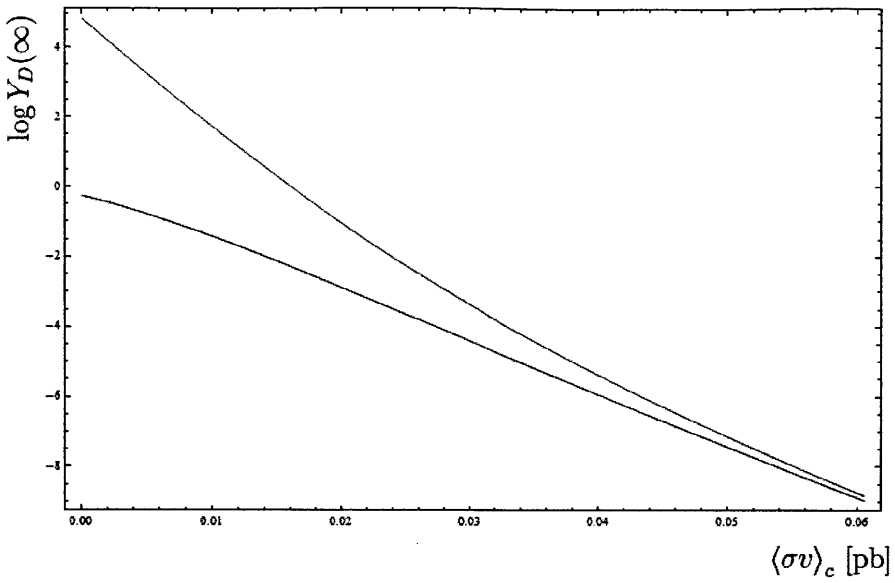


Figure 6-2: Dark matter abundance against catalytic cross section. The top curve is the relic abundance against catalytic cross section without any annihilation reaction. The bottom curve shows the relic abundance against catalytic cross section with an annihilation reaction of 0.12 pb. At very large catalytic cross sections, the two curves converge.

the annihilation reaction no matter how large the cross section is.

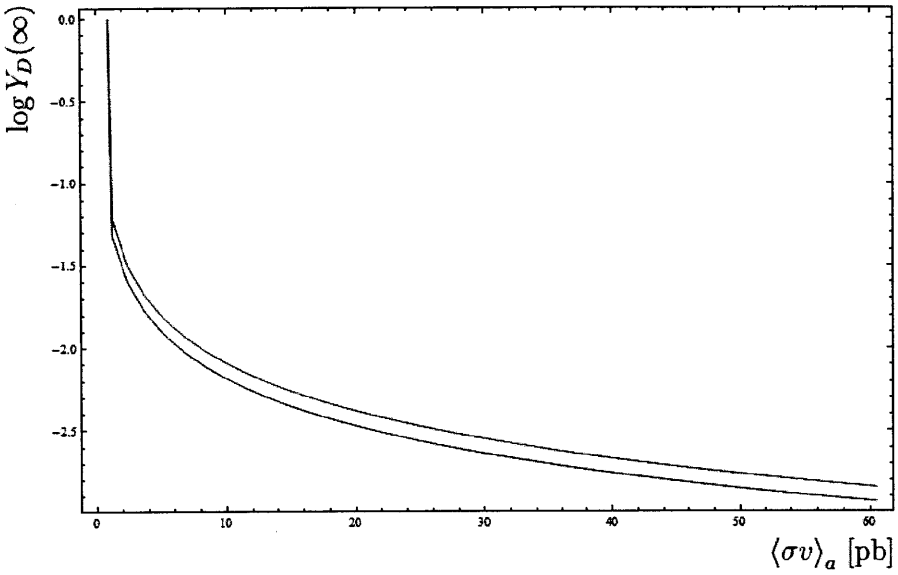


Figure 6-3: Dark matter abundance against annihilation cross section. The top curve is the relic abundance against annihilation cross section without any catalytic reaction. The bottom curve shows the relic abundance against annihilation cross section with a catalytic reaction of 0.0012 pb. Even at very large annihilation cross sections, the two curves do not converge.

# Chapter 7

# Physical Model

The toy model for catalytic dark matter analyzed in the previous sections is in fact motivated by supersymmetry (SUSY). In SUSY models, the following reaction can occur:

$$C + D \rightarrow C' + \phi \,, \tag{7.1}$$

$$C' + D \rightarrow C + \phi \,. \tag{7.2}$$

Here $\phi$ is a standard model particle such as a photon. $D$ is the supersymmetric partner of $\phi$. $C$ is some yet unobserved heavy particle, such as a fourth generation quark, and $C'$ its superpartner. It can be immediately seen that $Y_C + Y_{C'}$ is a constant, just like $Y_C$ in the toy model.

In our model, we would also like to enforce the triangle inequality between the masses of the three species $m_D$,$m_C$,$m_{C'}$, so that one does not decay into the other two, via, for example, $C' \rightarrow C + \bar{D} + \phi$. In particular, this requires $m_{C'} < m_C + m_D$ and all other permutations.

The above reactions are similar to the catalytic reaction analyzed in this paper, but to rigorously calculate the densities of each species, we would have to solve the Boltzmann equations with at least three species. That said, it is still reasonable to expect the general features of the catalytic toy model to hold.

As mentioned earlier, we assume both $C$ and $C'$ carry matter-antimatter asymme-

try, and they have both completely annihilated their respective anti-particles before the freeze-out of $D$ begins. However, we need to get rid of $C$ and $C'$ eventually, since we do not observe them today. In a typical SUSY model, there is a symmetry called $R$-parity, and $D$ is the lightest $R$-parity odd particle. If $C$ is $R$-parity even, then SUSY tells us that $C'$ is $R$-parity odd, and thus $C'$ must decay to the lightest $R$-parity odd particle, namely $D$, thus the relic abundance of $D$ will be enhanced by the decay of $C'$. On the other hand, $C$ can decay into standard model particles and won't affect dark matter abundance.

Since we are motivated by the baryon asymmetry to assume $Y'_C = 10^{-9}$, and the freeze-out density of $D$ is typically much lower ($\approx 10^{-11}$), we hope that the reactions will carry out in a way such that $C'+D \to C+\phi$ is more favorable than $C+D \to C'+\phi$ so that $Y_{C'}$ will be low enough in the end to not significantly increase $Y_D$ when $C'$ decays.

We argue that there are good reasons to believe this is the case. Assuming $C'$ and $C$ are kept in thermal equilibrium by the reactions (7.2), and that they are in the non-relativistic regime, the ratio of their equilibrium density can be approximated by equation 3.6 in [10]:

$$\frac{n_{C'}}{n_c} = \frac{g_{C'}(\frac{m_{C'}T}{2\pi})^{3/2}e^{-m_{C'}/T}}{g_C(\frac{m_CT}{2\pi})^{3/2}e^{-m_C/T}} = \left(\frac{m_{C'}}{m_C}\right)^{3/2} e^{-(m'_C-m_C)/T} . \tag{7.3}$$

The exponential term will dominate, so we can approximate the ratio between $C'$ and $C$ as $e^{-\Delta/T}$, where $\Delta$ is their mass difference. As long as $C'$ is more massive, the Boltzmann equation will favor the conversion of $C'$ to $C$, thus decreasing the density of $C'$. In other words, even though $C$ and $C'$ are not in thermal equilibrium with $\phi$, $C$ and $C'$ may be kept in relative equilibrium with each other.

The triangle inequality between $m_D$, $m_C$ and $m_{C'}$ implies that $\Delta = m_{C'} - m_C$ can be on the order of $m_D$. Recall we defined $x = m_D/T \approx \Delta/T$ in our Boltzmann equation, the density ratio $n_{C'}/n_C$ can be as small as $e^{-x}$. Since freeze-out occurs at $x \gg 1$, we expect only a very small amount of $C'$ in the end, which will not significantly increase the final yield for $D$ when it decays. However a more rigorous

calculation must be done to establish this claim.

The physical model based on SUSY reactions will likely preserve the properties of the catalytic reaction toy model. Additionally, the enhancement of the relic abundance due to the decay of $C'$ can be made insignificant by requiring $m'_C > m_C$.

# Chapter 8

# Conclusion

We studied a new type of reaction in the dark matter freeze-out calculation of the form $C+D \rightarrow C+\phi$. This catalytic reaction exhibits very different behavior than the standard annihilation reaction ($D + \bar{D} \rightarrow \phi + \phi$) since by assumption, the density of $C$ is constant, effectively making the Boltzmann equation for the density of $D$ linear. We found that by assuming $m_D = 100$ GeV, an ordinary annihilation cross section of 0.73 pb is required to make $\Omega_D h^2 = 0.1$. In the catalytic reaction, only a much smaller cross section of 0.02 pb is needed to get the same dark matter density.

We solved the Boltzmann equation for the catalytic reaction both numerically and analytically. The dynamics of the dark matter density differ from the annihilation case in two main ways:

1. It takes a much longer time for the dark matter density to stabilize.

2. The final abundance decreases much more sharply as we increase the catalytic cross section.

When both the catalytic and annihilation reactions are present, it is interesting to note that even if the catalytic reaction is very weak, it can still significantly affect the final abundance of dark matter, regardless of how big the annihilation cross section is. This means that catalytic reactions, if present, are crucial to calculating the relic abundance correctly, and may even dominate the annihilation reactions.

This form of catalytic reaction is natural in SUSY theories and can be applied with a very minor modification: instead of one catalytic species $C$, we will have $C$

and its superpartner $C'$, which undergo the following reactions.

$$C + D \rightarrow C' + \phi \,, \tag{8.1}$$

$$C' + D \rightarrow C + \phi \,. \tag{8.2}$$

As mentioned in section 7, the dynamics involving three species are slightly more complicated. In particular, since $C'$ will eventually decay into $D$, we need to include this effect in our calculation of the relic abundance.

Future work needs to be done to rigorously calculate $Y_{C'}$ and show that it can be neglected when dark matter freeze-out has occurred. Another issue not addressed in this paper is the dependence of various cross sections on time, which is assumed to be constant. An actual field theory model is needed to more rigorously establish the various results in this paper. Given the exciting prospects of detecting dark matter in the coming decade, it is crucial to theoretically study these variant dark matter scenarios.

# Bibliography


[1] G. Jungman, M. Kamionkowski, and K. Griest. *Supersymmetric dark matter, Phys. Rept. 267.* (1996) 195-373, hep-ph/9506380.

[2] L. Bergstrom. *Non-baryonic dark matter: Observational evidence and detection methods, Rept. Prog. Phys. 63.* (2000) 793, hep-ph/0002126.

[3] G. Bertone, D. Hooper, and J. Silk. *Particle dark matter: evidence candidates and constraints, phys. Rept. 405.* (2005) 279-390, hep-ph/0404175.

[4] M. Milgrom. *Astrophys. Journ. 270.* (1983).

[5] B. W. Lee and S. Weinberg. *Cosmological lower bound on heavy-neutrino masses, Phys. Rev. Lett. 39* (1977) 165-168.

[6] F. D'Eramo, J. Thaler. *Semi-annihilation of Dark Matter* JHEP **1006**, 109 (2010)

[7] K. Nakamura *et al.* (Particle Data Group), J. Phys. G **37**,075021 (2010)

[8] E. W. Kolb and M. S. Turner. *The Early Universe. Front. in Phys.* (1990).

[9] WMAP Collaboration. J.Dunkley *et al. Five-Year Wilkinson Microwave Anisotropy Probe (WMAP) Observations: Likelihoods and Parameters from the WMAP data, Astrophys. J. Suppl.* (2009) 306-329, arXiv: 0803.0586.

[10] S. Dodelson. *Modern Cosmology.* (2003).